

## Tunable terahertz wave generation in the 3- to 7-THz region from GaP

T. Tanabe<sup>a)</sup> and K. Suto

*Department of Materials Science, Graduate School of Engineering, Tohoku University, Aoba-yama 02, Sendai 980-8579, Japan*

J. Nishizawa

*Semiconductor Research Institute, Kawauchi, Aoba-ku, Sendai 980-0862, Japan*

K. Saito

*Department of Materials Science, Graduate School of Engineering, Tohoku University, Aoba-yama 02, Sendai 980-8579, Japan*

T. Kimura

*Semiconductor Research Institute, Kawauchi, Aoba-ku, Sendai 980-0862, Japan*

(Received 21 October 2002; accepted 19 May 2003)

Following the generation of tunable terahertz waves from GaP in the 0.5- to 3-THz region, we extended the frequency region up to 7 THz, using an optical parametric oscillator and a YAG laser (1.064  $\mu\text{m}$ ). The tuning angle  $\theta_{\text{in}}$  increased superlinearly in the 3- to 7-THz region, so that the total reflection took place at 5 THz, which was avoided by rotating the crystal relative to the incident optic axis. As a result, terahertz output peak powers of 100 mW at up to 5.6 THz and 3 mW at 7 THz were obtained, at pump and signal energies of 3 mJ, respectively. © 2003 American Institute of Physics. [DOI: 10.1063/1.1592889]

Nishizawa<sup>1,2</sup> predicted the generation of terahertz waves via the resonance of phonons and molecular vibrations. Subsequently, Nishizawa and Suto<sup>3</sup> realized a semiconductor GaP Raman laser and generated a 12-THz wave with a peak power as high as 3 W using a GaP Raman oscillator containing a GaAs mixing crystal.<sup>4</sup> Loudon made a similar proposal, although he thought that a uniaxial crystal was required.<sup>5,6</sup> High-power, frequency-tunable THz-wave sources can be used for linear far-infrared spectral measurements of macromolecules, such as polymers, biomolecules (e.g., glucose, DNA), vibration-induced chemical reactions, and as the local oscillator for heterodyne detection at THz-frequency region. Thus, Nishizawa promoted the development of THz-wave generation utilizing lattice resonance, and proposed applying wavelength-tunable THz waves to the detection and treatment of cancer.<sup>7</sup> Under his guidance, Kawase *et al.*<sup>8</sup> recently reported frequency-tunable, high-power THz-wave generation. They obtained a maximum energy of 1.3 nJ/pulse (peak power of 200 mW) at 1 THz, by adopting injection seeding in LiNbO<sub>3</sub>. Bakker *et al.* reported THz-wave generation via excitation of phonon polaritons in LiNbO<sub>3</sub> (1-4.8 THz).<sup>9</sup> Zhang *et al.* reported THz-wave generation using difference-frequency generation (DFG) with femtosecond pulses,<sup>10,11</sup> and THz imaging of biological tissues as one of the applications of the THz-wave.<sup>12,13</sup>

Other THz-wave sources, such as free electron laser,<sup>14</sup> *p*-Ge laser,<sup>15</sup> quantum cascade laser,<sup>16</sup> photomixer,<sup>17</sup> and backward wave oscillator,<sup>18</sup> have been developed. In comparison to these sources, the THz-wave source based on the DFG is useful in terms of operation at room temperature, scale of the apparatus, and continuous tunability.

We first realized Raman lasing oscillation via the polar-

iton mode in GaP.<sup>3,19</sup> Exact collinear phase matching of the difference wave in GaP was obtained at wavelengths shorter than 990 nm.<sup>20</sup> We recently generated frequency-tunable, high-power THz waves in the region from 0.5 to 3 THz from GaP, using an optical parametric oscillator (OPO) and a 1.064- $\mu\text{m}$  YAG laser, under small-angle noncollinear phase-matching conditions.<sup>21</sup> The maximum THz energy was 2.88 nJ/pulse (480 mW) at 1.3 THz for OPO and YAG laser energies of 5.8 and 26 mJ, respectively.

This letter describes, tunable, THz-wave generation in the frequency range from 3 to 7 THz from GaP, under small-angle, noncollinear phase-matching conditions.

The two lasers used for DFG in GaP were a 1.064- $\mu\text{m}$  YAG laser and a  $\beta$ -BaB<sub>2</sub>O<sub>4</sub>-based OPO pumped by the 355 nm (third-harmonic) beam from the YAG laser. Both lasers ran at a repetition rate of 10 Hz. Details of the experimental setup used in the present work are given elsewhere.<sup>21</sup> The pulse energies of the YAG and OPO were both attenuated to 3 mJ before incidence on the GaP crystal. Their pulse widths were 11 and 6 ns, respectively.

Semi-insulating GaP crystals were shaped into rectangles 2.6 or 5 mm long in the  $\langle 110 \rangle$  direction and 3 mm thick in the  $\langle 001 \rangle$  direction. The signal beam from the YAG laser was combined with the pump beam from the OPO using a polarizing cube beam splitter. The incident beams roughly paralleled the  $\langle 110 \rangle$  crystal direction of GaP. The wavelength of the OPO was varied between 1.03 and 1.06  $\mu\text{m}$ . The THz-wave output was collected using paraboloid reflectors and detected with a liquid-helium-cooled Si bolometer (Infrared Laboratories, Inc., USA). The bolometer signal was measured with a digital oscilloscope. The response time of the bolometer is 100  $\mu\text{s}$ . The sensitivity of the bolometer is  $2.57 \times 10^5$  V/W.

Figure 1 shows the frequency dependence of the THz-wave maximum output energy at various  $\theta_{\text{in}}^{\text{ext}}$ , where  $\theta_{\text{in}}^{\text{ext}}$  is

<sup>a)</sup>Author to whom correspondence should be addressed; electronic mail: tanabet@material.tohoku.ac.jp

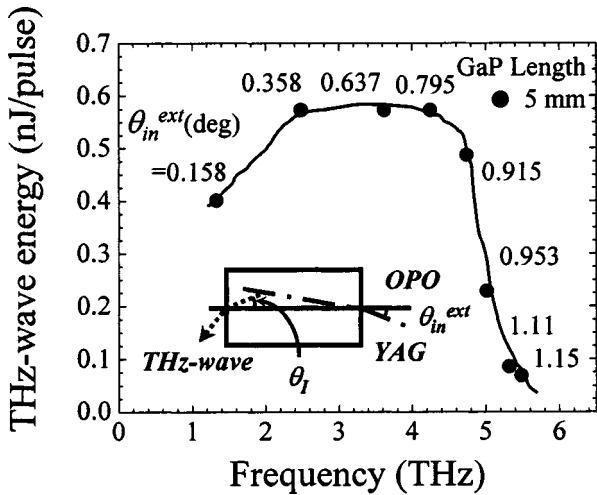


FIG. 1. Frequency dependence of the THz-wave output energy at various  $\theta_{in}^{ext}$  in GaP crystals. The incident pump beam was nearly normal to the GaP surface ( $\alpha^{ext} \approx 0$ ).

the external angle between the pump and signal beams outside the GaP crystal. THz waves from 1 to 5.5 THz were generated. In this measurement, the GaP crystal was 5 mm long and the pump beam was incident nearly normal to the crystal surface. The THz-wave energy remained at about 0.6 nJ/pulse (peak power of 100 mW) over a wide frequency range (2.5–4.3 THz). The THz-wave energy in the 4.5–5.5-THz frequency region decreased rapidly. For  $\theta_{in}^{ext} > 1.17^\circ$ , no THz-wave power was detected in this configuration.

However, for THz-wave frequencies higher than 5.5 THz ( $\theta_{in}^{ext} > 1.17^\circ$ ), a much higher power was obtained by rotating the GaP crystal relative to the pump beam. Figure 2 shows that the THz-wave output ranged from 5.5 to 7.5 THz in this configuration. For  $\theta_{in}^{ext} = 1.23^\circ$ , at which the THz-wave frequency was 5.65 THz, the output energy increased to 0.6 nJ/pulse (peak power of 100 mW) when the incident angle of the pump beam from the surface normal ( $\alpha^{ext}$ ) was set at  $15^\circ$ . With further increase in  $\theta_{in}^{ext}$ , the output energy decreased to 0.018 nJ/pulse at 7 THz ( $\theta_{in}^{ext} = 2.77^\circ$ ,  $\alpha^{ext} = 34^\circ$ ). For THz-wave frequencies above 7 THz, the 2.6-

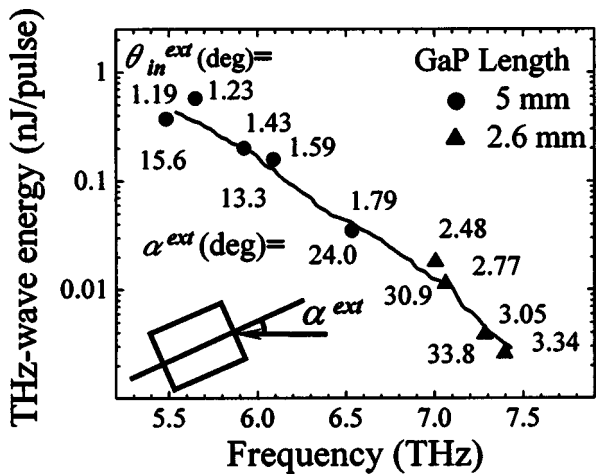


FIG. 2. Frequency dependence of the THz-wave output energy at various  $\theta_{in}^{ext}$  in GaP crystals. The GaP crystal was rotated  $\alpha^{ext}$ . The incident pump beam was diagonal to the GaP surface.

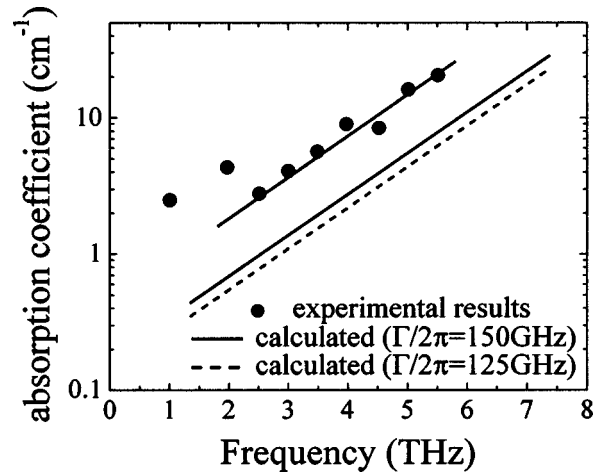


FIG. 3. Absorption coefficient spectrum of GaP in the region from 1 to 5.5 THz.

mm-long crystal gave higher energy than the 5-mm-long crystal.

In our previous work,<sup>21</sup> we discussed the phase-matching condition for noncollinear interactions inside a GaP crystal, and showed that  $\sin \theta_l \approx \sqrt{2\Delta q/q}$ , where  $q$  is the wave vector of a THz wave and  $\Delta q$  is the deviation of  $q$  in the collinear configuration from the exact collinear phase-matching value.  $\theta_l$  is the angle inside the GaP crystal between the THz wave and the YAG laser beam directions. For THz-wave generation from 1 to 5 THz (Fig. 1), the deviation ( $\Delta q/q$ ) is so small that the THz wave generated in GaP is not totally reflected, and leaves via the GaP crystal end-surface. When THz waves are generated in the frequency range above 5 THz (Fig. 2), the deviation increases considerably because of the dispersion curve of the polariton branch of GaP.

At 5 THz, the wave number mismatch ( $\Delta q/q$ ) is calculated to be 0.0519;<sup>21</sup>  $\theta_l$  is then calculated to be  $20.9^\circ$  from the aforementioned equation, while it was estimated to be  $17.8^\circ$  from the measurement of the THz beam direction angle outside the crystal  $\theta_{in}^{ext}$ . These are close to the critical angle of the total reflection,  $18.9^\circ$ . Therefore, we rotated the GaP crystal to prevent total internal reflection (see the inset of Fig. 2). As a result, the THz output extended above 7 THz. These results indicate that the frequency of the THz wave can be tuned continuously by changing the phase-matching angle  $\theta_{in}^{ext}$ .

The THz-wave absorption coefficient of GaP was measured in the region from 1 to 5.5 THz using the emitted THz wave, as shown in Fig. 3. The THz-wave linewidth used for this measurement was measured to be 3.27 GHz (at 1.01 THz) using a far-infrared Fabry–Perot interferometer.<sup>22</sup> This linewidth is determined by the linewidth of the pump light. In this measurement, we prepared other semi-insulating GaP crystals with thicknesses of 1, 1.2, 2.6, and 5 mm and measured the absorption coefficient using the output THz power from the GaP crystal as a source with a single-beam method. This result is consistent with a reference data.<sup>23</sup> Above 3 THz, it increased steeply along with the calculated coefficient for lattice resonance with  $\Gamma/2\pi = 370$  GHz, where  $\Gamma$  is the damping constant of the lattice resonance. This value is 2.5 times that of the TO phonon observed for backward

Raman scattering in high-purity GaP epitaxial layers ( $\Gamma/2\pi = 125\text{--}150$  GHz). This discrepancy and the residual absorption at low frequency may have been caused by imperfections in semi-insulating GaP crystals, or by multiphonon absorption. From Fig. 3, the absorption coefficient is as large as  $50\text{ cm}^{-1}$  at 7 THz, which is one of the reasons for the decrease in the THz power at this frequency.

In conclusion, a continuously frequency-tunable THz wave up to 7.4 THz was generated in GaP crystals. In our study, the THz-wave energy was as high as 0.6 nJ/pulse (peak power of 100 mW) in the frequency range 2.5–5.7 THz and 0.018 nJ/pulse (peak power of 3 mW) at 7 THz, at pump and signal energies of 3 mJ. By using GaP with a more perfect crystal, higher power and a wider frequency range of the THz-wave generation would be expected. In addition, we can get higher efficiency by reducing the incident beam diameter if we can get higher damage-threshold crystals.

This work was supported by a Grant-in-Aid for Creative Scientific Research (No. 13GS0002) from the Japan Society for the Promotion of Science.

<sup>1</sup>J. Nishizawa, *Denshi Kagaku* **14**, 17 (1963) (in Japanese).

<sup>2</sup>J. Nishizawa, *Denshi Gijutu* **7**, 101 (1965) (in Japanese).

<sup>3</sup>J. Nishizawa and K. Suto, *J. Appl. Phys.* **51**, 2429 (1980).

<sup>4</sup>K. Suto and J. Nishizawa, *IEEE J. Quantum Electron.* **QE-19**, 1251 (1983).

<sup>5</sup>R. R. Loudon, *Proc. Phys. Soc. London* **82**, 393 (1963).

<sup>6</sup>J. M. Yarborough, S. S. Sussman, H. E. Purhoff, R. H. Pantell, and B. C. Johnson, *Appl. Phys. Lett.* **15**, 102 (1969).

<sup>7</sup>J. Nishizawa, *J. Acoust. Soc. Jpn.* **57**, 163 (2001).

<sup>8</sup>K. Kawase, J. Shikata, K. Imai, and H. Ito, *Appl. Phys. Lett.* **78**, 2189 (2001).

<sup>9</sup>H. J. Bakker, S. Hunsche, and H. Kurz, *Phys. Rev. B* **50**, 914 (1994).

<sup>10</sup>A. Rice, Y. Jin, X. F. Ma, X.-C. Zhang, D. Bliss, J. Larkin, and M. Alexander, *Appl. Phys. Lett.* **64**, 1324 (1994).

<sup>11</sup>D. H. Auston and M. C. Nuss, *IEEE J. Quantum Electron.* **QE-24**, 184 (1988).

<sup>12</sup>P. Y. Han, G. C. Cho, and X.-C. Zhang, *Opt. Lett.* **25**, 242 (2000).

<sup>13</sup>B. Ferguson and X.-C. Zhang, *Nature Materials* **1**, 26 (2002).

<sup>14</sup>G. Ramian, J. Kaminski, and S. J. Allen, *Nucl. Instrum. Methods Phys. Res. A* **393**, 220 (1997).

<sup>15</sup>S. Komiyama, *Phys. Rev. Lett.* **48**, 271 (1982).

<sup>16</sup>J. Faist, F. Capasso, D. L. Sivco, C. Sirtori, A. L. Hutchinson, and A. Y. Cho, *Science* **287**, 553 (1994).

<sup>17</sup>E. B. Brown, K. A. McIntosh, K. B. Nichols, and C. L. Dennis, *Appl. Phys. Lett.* **66**, 285 (1995).

<sup>18</sup>A. Volkov, *Int. J. Infrared Millim. Waves* **8**, 55 (1987).

<sup>19</sup>J. Nishizawa and K. Suto, in *Infrared and Millimeter Waves 7*, edited by K. J. Button (Academic, New York, 1983), pp. 301–320.

<sup>20</sup>T. Taniuchi, J. Shikata, and H. Ito, *8th IEEE International Conference on Terahertz Electronics 2000*, paper P-8, p. 225.

<sup>21</sup>T. Tanabe, K. Suto, J. Nishizawa, T. Kimura, and K. Saito, *J. Appl. Phys.* **93**, 4610 (2003).

<sup>22</sup>T. Tanabe, K. Suto, J. Nishizawa, K. Saito, and T. Kimura (unpublished).

<sup>23</sup>E. D. Palik, *Handbook of Optical Constants of Solids* (Academic, Orlando, 1985), Vol. 1.